ELSEVIER

Urologic Oncology: Seminars and Original Investigations 000 (2018) 1–9

UROLOGIC ONCOLOGY

Original Article

Predicting the tumorigenic phenotype of human bladder cancer cells by combining with fetal rat mesenchyme

Manabu Miki, M.D.[a,1], Kenichiro Ishii, Ph.D.[a,b,1], Takeshi Sasaki, M.D., Ph.D.[a], Manabu Kato, M.D., Ph.D.[a], Shinya Kajiwara, M.D.[a], Hideki Kanda, M.D., Ph.D.[a], Kiminobu Arima, M.D., Ph.D.[a], Yoshifumi Hirokawa, M.D., Ph.D.[b], Masatoshi Watanabe, M.D., Ph.D.[b], Yoshiki Sugimura, M.D., Ph.D.[a,*]

[a] *Department of Nephro-Urologic Surgery and Andrology, Mie University Graduate School of Medicine, Mie, Japan*
[b] *Department of Oncologic Pathology, Mie University Graduate School of Medicine, Mie, Japan*

Received 24 April 2018; received in revised form 10 July 2018; accepted 14 July 2018

Abstract

Background: In nonmuscle invasive bladder cancer patients, prediction of pTa and pT1 bladder cancer recurrence and progression must be established. Micropapillary structures have been defined as small clusters of invasive cancer cells having features of the epithelial-mesenchymal transition. Since the stromal microenvironment helps to induce the epithelial-mesenchymal transition, interactions between cancer cells and stroma should be closely examined to predict the tumorigenic phenotype of human bladder cancer cells.

Materials and methods: To investigate differences in the responsiveness of cancer cells to stroma, we combined 3 established human bladder cancer cell lines (high-grade T24 and UM-UC-3 cells, and low-grade papillary RT4 cells) with fetal rat mesenchyme.

Results: Among 3 bladder cancer cell lines, the expression profiles of p63 isoforms were distinct, i.e., p63γ in T24 cells, p63β in UM-UC-3 cells, and p63α in RT4 cells. Tumors formed by T24 cells combined with fetal mesenchyme formed micropapillary-like structures, whereas those formed by T24 cells alone did not. T24 cells combined with fetal mesenchyme showed poor differentiation, e.g., innumerable chromatic atypia in the nuclei, higher levels of chromatic condensation, and increased nucleoli. In contrast, both UM-UC-3 and RT4 cells combined with fetal mesenchyme did not form micropapillary-like structures. Ki-67 and p63 labeling indices were significantly elevated by combining fetal mesenchyme with T24 cells but not with the others.

Conclusions: By mixing cancer cells with fetal mesenchyme, our data demonstrated that formation of micropapillary-like structures may predict the tumorigenic phenotype of invasive bladder cancer cells. Taken together, distinct expression profiles of p63 isoforms may predict poor outcomes in invasive bladder cancer. © 2018 Published by Elsevier Inc.

Keywords: Invasive bladder cancer; Responsiveness of cancer cells to stroma; Fetal mesenchyme; Micropapillary-like structures; p63 isoforms

Abbreviations: BLM, bladder mesenchyme; CIS, carcinoma in situ; EMT, epithelial-mesenchymal transition; H&E, hematoxylin and eosin; MIBC, muscle invasive bladder cancer; MVD, microvessel density; NMIBC, nonmuscle invasive bladder cancer; TUR, transurethral resection; UGM, urogenital sinus mesenchyme.

1. Introduction

Most bladder cancers are urothelial carcinomas. Roughly 75% of patients have nonmuscle invasive bladder cancer (NMIBC) and the remainder have muscle invasive or metastatic disease [1]. For all stages, the 5-year relative survival is around 70% to 80% [2]. The rate of recurrence in NMIBC ranges from 50% to 90%. In addition, 10% to 30% of NMIBC patients progress to muscle invasive bladder cancer (MIBC) requiring radical surgery [1]. In NMIBC patients after first transurethral resection, identification of the key predictors of progression should improve overall survival by supporting the use of aggressive treatment in short-term follow-up. Identifying NMIBC with poor

*Corresponding author. Tel.: +81-59-231-5026; fax: +81-59-231-5203.
E-mail address: sugimura@clin.medic.mie-u.ac.jp (Y. Sugimura).
[1]These authors contributed equally to this work.

https://doi.org/10.1016/j.urolonc.2018.07.008
1078-1439/

outcomes at the first admission is not an easy task. Thus, follow-up exams that predict pTa and pT1 bladder cancer recurrence and progression must be established for these patients.

As carcinomas progress, tumors may lose epithelial morphology and acquire mesenchymal characteristics. This is called the epithelial-mesenchymal transition (EMT) and is known to play an important role during this process [3]. The EMT is a highly conserved process in which polarized immotile epithelial cells transition to motile mesenchymal cells. Histopathologically, micropapillary structures such as tumor budding are defined as small clusters of undifferentiated cancer cells like mesenchymal-transitioned cancer cells at the invasive front of tumor tissue [4]. These structures reflect the detachment of cancer cells and are associated with the EMT [5]. In bladder cancer, there are few reports of clinical specimens that have been used to assess the importance of micropapillary structures [6,7].

Cancer cells directly influence their surrounding stroma through invasion [8]. When cancer cells co-opt stromal cells, tumor−stromal interactions likely activate cancer cells, promoting acquisition of invasive traits [9]. The responsiveness of cancer cells to stroma is therefore critical to tumor progression, including invasion. Here, we focused on the interactions between cancer cells and stroma, with an emphasis on identifying new predictors of poor outcomes in invasive bladder cancer. Indeed, it was reported that a highly invasive bladder cancer cell line seeded onto a living culture of bladder fibroblasts infiltrated the fibroblast layer and showed marked stimulation [10]. In contrast, a low-grade papillary bladder cancer cell line did not show these responses. Thus, differences in the responsiveness of cancer cells to stroma might point to new predictors of poor outcomes in invasive bladder cancer.

Bladder cancers can be grouped on the basis of gene expression patterns into basal and luminal subtypes, similar to the corresponding subtypes of breast cancer [1]. Studies in preclinical models suggest that basal and luminal bladder cancers arise from different progenitor or stem cells in the normal urothelium [11,12]. Bladder cancer develops via 2 distinct but somewhat overlapping tracks referred to as papillary and nonpapillary that represents two clinically and pathogenetically distinct forms of the disease [13]. In normal bladder, the nuclei of basal and intermediate cell layers are positive for expression of p63, CK5, and CK14. In NMIBC, almost 100% of cancer cells were positive for total p63 using anti-p63 antibodies (clone 4A4) [14]. In contrast, the p63 labeling index was significantly lower in pT2 MIBC, suggesting that the basal-like phenotype in cancer cells may disappear during bladder cancer progression, having features of the EMT.

To investigate differences in the responsiveness of cancer cells to stroma, an experimental in vivo model was developed. EMT-related growth factors such as epidermal growth factor and fibroblast growth factors are produced by fetal mesenchyme [15]. Here, embryonic rat urogenital sinus mesenchyme (UGM) and bladder mesenchyme (BLM) were used as sources of fetal mesenchyme, i.e., undifferentiated fibroblasts that induce or permit development and differentiation in prostate and bladder [16,17]. In this study, we combined 3 established human bladder cancer cell lines (high-grade T24 and UM-UC-3 cells, and low-grade papillary RT4 cells) with UGM or BLM. We then histopathologically evaluated the tumorigenic phenotypes of the 3 established human bladder cancer cell lines, focusing on the formation of micropapillary-like structures.

2. Materials and methods

2.1. Antibodies

Mouse monoclonal anti-E-cadherin antibodies (clone 36/E) were purchased from BD Transduction Laboratories (San Jose, CA). Rabbit polyclonal anticow cytokeratin wide spectrum screening (WSS), mouse monoclonal anti-p63 (clone 4A4), and mouse monoclonal antihuman-specific Ki-67 antigen (clone MIB-1) antibodies were purchased from DakoCytomation, Inc. (Copenhagen, Denmark). Mouse monoclonal antiactin, α-smooth muscle (α-SMA) (clone 1A4) and mouse monoclonal-anti-β-actin (clone AC-15) antibodies were purchased from Sigma-Aldrich Co., LLC. (St. Louis, MO).

2.2. Cell culture

Human bladder cancer T24, UM-UC-3, and RT4 cell lines were obtained from the American Type Culture Collection (Rockville, MD). T24 cells were cultured in minimum essential medium Eagle with 10% fetal bovine serum (FBS). UM-UC-3 cells were cultured in Eagle's minimum essential medium with 10% FBS. RT4 cells were cultured in McCoy's 5A medium with 10% FBS.

2.3. Preparation of cell lysates and Western blot analysis

Subconfluent cultured T24, UM-UC-3, and RT4 cells were harvested by scraping, and whole cell lysates were prepared as previously described [18]. Equal amounts of extracted protein (40 μg) were separated by gel electrophoresis and transferred to immobilon polyvinylidene difluoride membranes following our previously reported protocol [19]. Specific protein bands were detected with a LAS-4000 Mini (Fuji Photo Film, Tokyo, Japan) using anti-E-cadherin (1:5000), anti-p63 (1:200), or anti-β-actin (1:5000) antibodies.

2.4. Animal studies

Eight to 9-week-old severe combined immune-deficient male mice and pregnant Sprague-Dawley (SD) rats were purchased from Japan SLC, Inc. (Hamamatsu, Japan). All animals were maintained in a specific pathogen-free environment under controlled conditions of light and humidity.

Food and tap water were provided ad libitum. The Mie University's Committee on Animal Investigation approved the experimental protocol.

2.5. Preparation of mixed cultures composed of human bladder cancer cells and fetal rat UGM and BLM

Fetal rat UGM and BLM were prepared from 17-day-old SD rat fetuses (plug date denoted as day 0) as previously described [20]. Urogenital sinuses were dissected from the fetuses and separated into epithelial and mesenchymal components by tryptic digestion and mechanical separation. BLM was isolated from bladder samples by incubation with 20 mM ethylenediaminetetraacetic acid in calcium and magnesium-free Hank's solution at room temperature for 60 minutes, followed by mechanical separation of epithelium and stroma. Both UGM and BLM were then further digested to single-cell suspensions by 60-minutes digestion at 37 ˚C with 187 units/ml collagenase (Gibco-BRL, Grand Island, NY). Following digestion, the cells were extensively washed with RPMI 1640 medium with 5% FBS. Viable cells were then counted after trypan blue staining using a hemocytometer.

Subconfluent cultures of T24, UM-UC-3, or RT4 cells were trypsinized and counted with a hemocytometer. Mixed cultures consisting of UGM or BLM were prepared by mixing 5×10^5 cancer cells and 1×10^5 UGM or BLM in suspension. Xenografts without UGM or BLM contained only 5×10^5 cancer cells. Pelleted cells were resuspended in 50 μL neutralized type I rat tail collagen gels, and then grafted beneath the renal capsule of 36 severe combined immunedeficient mice (3 cancer cell lines x 3 groups x 4 mice). In this study, 1 or 2 xenografts were implanted per kidney, meaning that the n numbers were varied between 10 and 16. After xenografting, mice were killed at 4 weeks, and grafts were harvested.

2.6. Immunohistochemistry

Endogenous peroxidase activity was blocked with 0.3% hydrogen peroxide in methanol for 20 minutes. Antigen retrieval was performed using 10 mM sodium citrate buffer of pH 6.0 for Ki-67. Antigen Unmasking Solution (Vector laboratories Inc., Burlingame, CA) was used for WSS and p63. For αSMA, antigen retrieval was not performed. After incubation with primary antibodies, sections were incubated with appropriate biotinylated secondary antimouse or antirabbit immunoglobulin included in the ImmPRESS Reagent Kit (Vector Laboratories, Inc.) for 30 minutes at room temperature. The antigen-antibody reaction was visualized using 3,3′-diaminobenzidine tetrahydrochloride as a substrate. Sections were counterstained with hematoxylin and examined by light microscopy. Anti-Ki-67 and anti-p63 antibodies were used at dilutions of 1:300. Anti-WSS and anti-αSMA antibodies were used at dilutions of 1:1000 and 1:10000, respectively.

Cell proliferation of WSS-positive human bladder cancer cells in xenografted tumors was determined by the percentage of Ki-67-positive nuclei in 10 separate microscopic fields at × 400 magnification from each tissue specimen. The p63 labeling index of WSS-positive human bladder cancer cells in xenografted tumors was determined by the percentage of p63-positive nuclei in 10 separate microscopic fields at × 400 magnification from each tissue specimen.

2.7. Statistical analysis

Data are presented as the mean ± SD. Statistically significant differences between two groups were determined using Student's t test. Values of $P < 0.05$ were considered statistically significant.

3. Results

3.1. Characteristics of 3 human bladder cancer cell lines in vitro

High-grade T24 and UM-UC-3 cells were spindle-shaped single cells without well-defined cell−cell contacts (Fig. 1A). They did not express E-cadherin protein (Fig. 1B). In contrast, low-grade papillary RT4 cells grew as flat islands of polygonal-shaped cells with well-defined cell−cell contacts (Fig. 1A). They expressed an abundant level of E-cadherin protein (Fig. 1B). As shown in Fig. 1B, all 3 cancer cell lines were positive for p63 protein. The expression profiles of p63 isoforms were distinct, i.e., p63γ in T24 cells, p63β in UM-UC-3 cells, and p63α in RT4 cells.

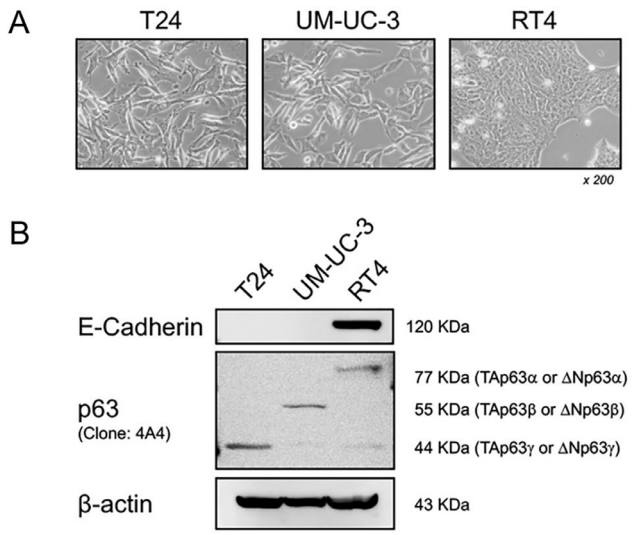

Fig. 1. Characteristics of 3 human bladder cancer cell lines. (A) Cell morphologies of T24, UM-UC-3, and RT4 cells in vitro. Magnification = × 200. (B) Protein expression profiles of 3 human bladder cancer cell lines. Equal amounts of protein (40 μg) were electrophoresed, transferred to immobilon polyvinylidene difluoride membranes, and incubated with antibodies for E-cadherin and p63. Proteins were visualized with horseradish peroxidase (HRP)-conjugated secondary antibodies and chemiluminescence. Adequate loading was confirmed by blotting for β-actin.

Table 1
Combination of fetal mesenchyme with human bladder cancer cells: effects on recovery rates in xenografted tumors

Cell line	Recovery rate (%)		
	Alone	+ UGM	+ BLM
T24	100 ($n = 15$)	100 ($n = 16$)	100 ($n = 11$)
UM-UC-3	100 ($n = 12$)	100 ($n = 10$)	100 ($n = 11$)
RT4	100 ($n = 13$)	79 ($n = 14$)	93 ($n = 14$)

3.2. Combining 3 human bladder cancer cell lines with fetal mesenchyme: Effects on recovery rates and tumor growth in vitro

The recovery rates of T24 cells or UM-UC-3 cells mixed with fetal mesenchyme such as UGM and BLM were 100%, whereas those of RT4 cells mixed UGM or BLM were 79% or 93%, respectively (Table 1).

In T24 cells + fetal mesenchyme groups, the tumor weights of T24 cells + the UGM group was significantly heavier than those of T24 cells + the BLM group (Fig. 2a). In contrast, no significant difference of tumor weights was observed when UM-UC-3 cells or RT4 cells were grafted with fetal mesenchyme (Fig. 2b and c). Of note, the total cell number in xenografts was clearly different in this study, i.e., xenografts with UGM or BLM contained 5×10^5 cancer cells and 1×10^5 UGM or BLM, and xenografts without UGM or BLM contained only 5×10^5 cancer cells.

3.3. Histopathological characteristics of T24 cells mixed with fetal mesenchyme in vivo

T24 cells mixed with or lacking fetal mesenchyme (UGM and BLM) formed solid white tumors of spheroidal or irregular shapes (Fig. 3a–c). When T24 cells were inoculated alone, the resultant tumors consisted almost entirely of cancer cells as determined by H&E staining (Fig. 3d). In contrast, abundant stroma and micropapillary-like structures of cancer cells were shown in the T24 cells + fetal mesenchyme groups (Fig. 3e and f). WSS-positive T24 cells surrounded by αSMA-positive smooth muscle cells or myofibroblasts were observed (Fig. 3h, i, k, and l). As compared to T24 cells inoculated alone, poorly differentiated cancer cells were increased in T24 cells + fetal mesenchyme groups. T24 cells + fetal mesenchyme groups also exhibited innumerable chromatic atypias in the nuclei, higher level of chromatic condensation, and increased nucleoli.

3.4. Histopathological characteristics of UM-UC-3 combined with fetal mesenchyme in vivo

The gross appearance of UM-UC-3 cells mixed with or lacking fetal mesenchyme showed reddish solid tumors with poorly defined margins (Fig. 4a–c). H&E staining of xenografted tumors revealed necrotic compartments and large blood-filled spaces in UM-UC-3 cells with or without fetal mesenchyme groups (Fig. 4d–f). In UM-UC-3 cells + fetal mesenchyme groups, there was little stroma in the tumors, i.e., micropapillary-like structures were not formed (Fig. 4e and f). Weak and irregular staining for WSS was observed in most regions of UM-UC-3 cells (Fig. 4g–i) and neither αSMA-positive smooth muscle cells nor myofibroblasts were observed (Fig. 4j–l). In UM-UC-3 tumors with or without fetal mesenchyme, no strict polarity was observed; poorly differentiated cells with large or small pleomorphic nuclei were observed.

3.5. Histopathological characteristics of RT4 mixed with fetal mesenchyme in vivo

Transplanted RT4 cells combined with or lacking fetal mesenchyme generated white solid tumors of spheroidal or

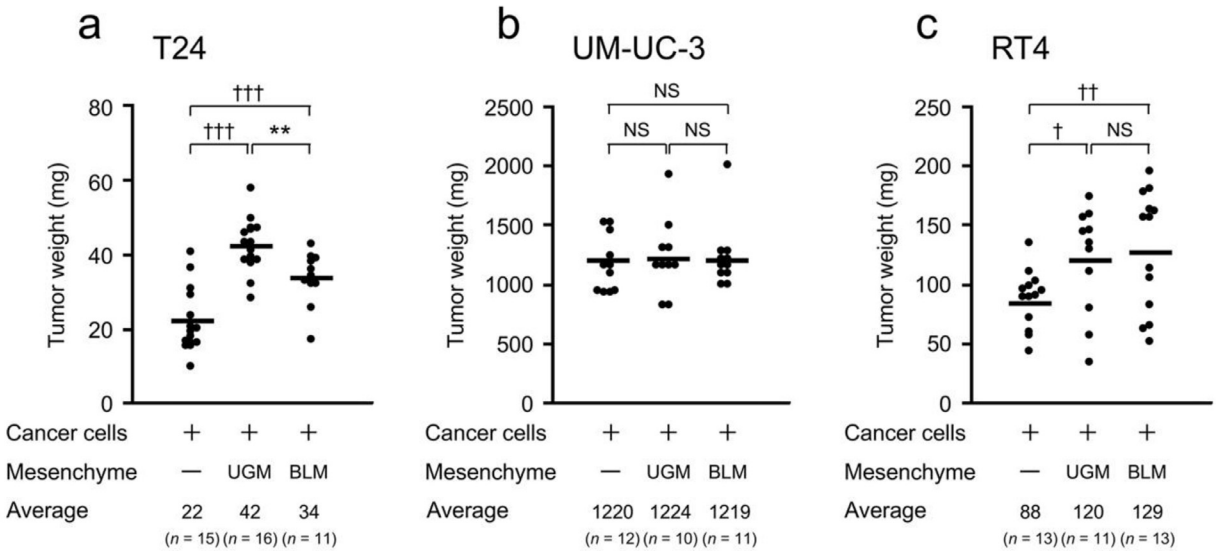

Fig. 2. Combination of fetal mesenchyme with human bladder cancer cells: effects on tumor growth in xenografted tumors. Tumor weights of T24 cells (a), UM-UC-3 cells (b), and RT4 cells (c) were measured on day 28 after xenografting. $^{**}P < 0.01$ vs. cancer cells + UGM. $^{\dagger}P < 0.05$, $^{\dagger\dagger}P < 0.01$, $^{\dagger\dagger\dagger}P < 0.001$ vs. cancer cells alone. NS, not significant.

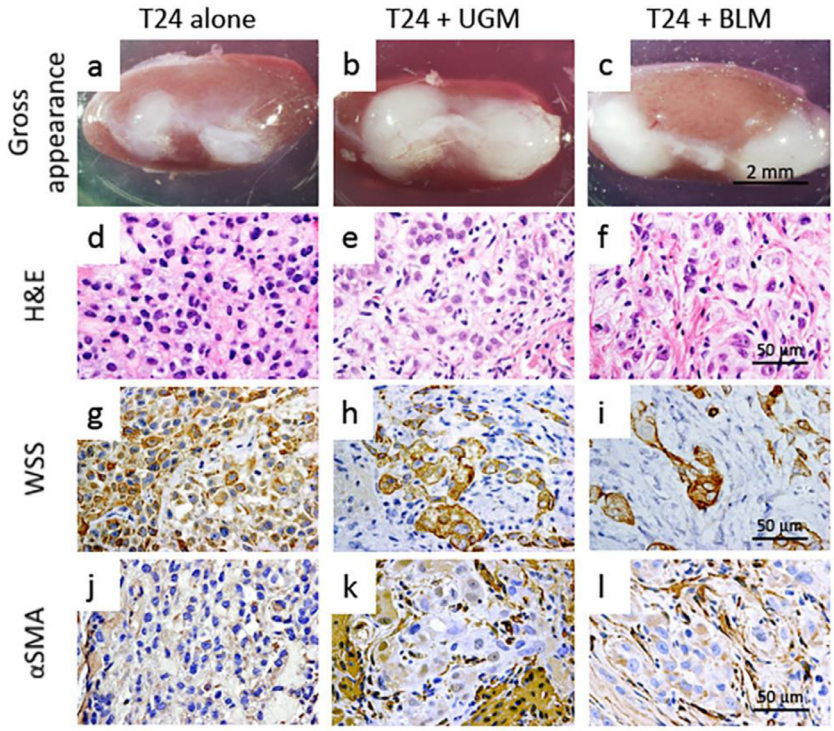

Fig. 3. Mixtures of fetal mesenchyme and T24 cells: effects on tumorigenic phenotype. (a–c) Gross appearances of T24 cells inoculated alone and T24 cells plus fetal mesenchyme (bar = 2 mm). Representative images of H&E stained tissue (d–f), WSS staining (g–i), and αSMA staining (j–l) (bar = 50 μm, magnification = × 400).

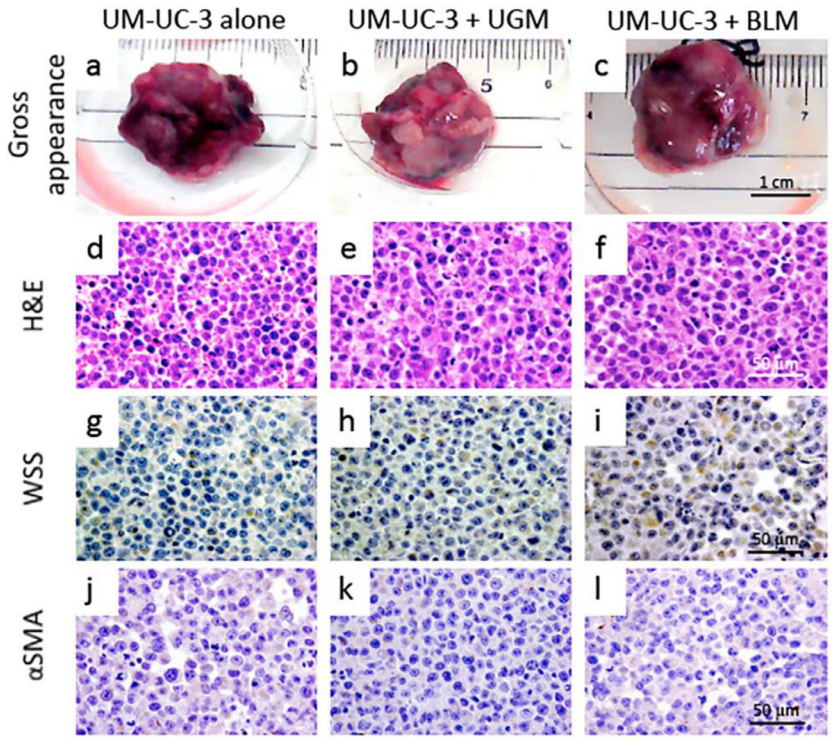

Fig. 4. Mixtures of fetal mesenchyme and UM-UC-3 cells: effects on tumorigenic phenotype. (a–c) Gross appearances of UM-UC-3 cells inoculated alone and UM-UC-3 cells plus fetal mesenchyme (bar = 1 cm). Representative images of H&E stained tissue (d–f), WSS staining (g–i), and αSMA staining (j–l) (bar = 50 μm, magnification = × 400).

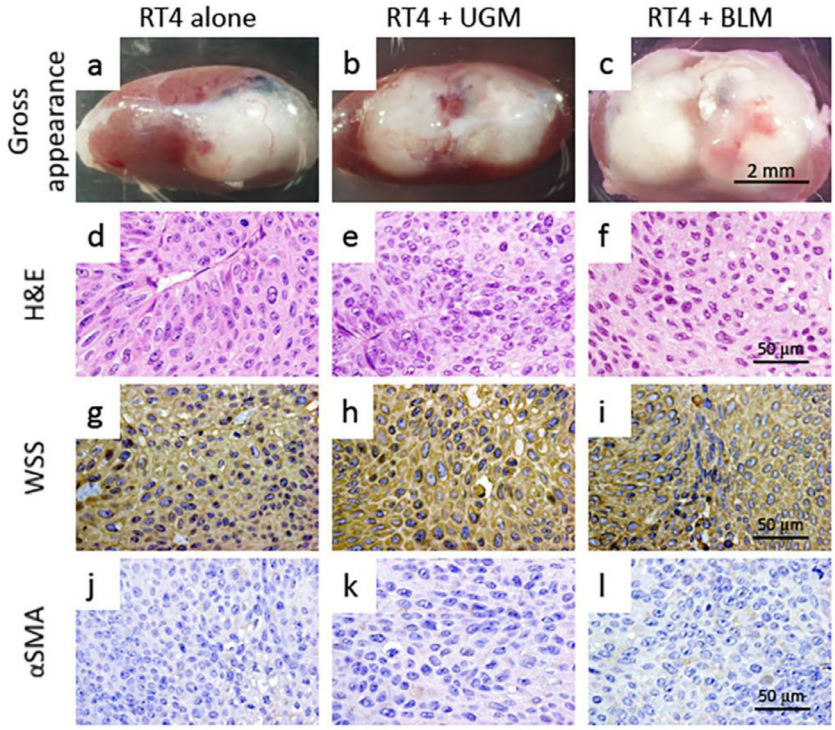

Fig. 5. Mixtures of fetal mesenchyme and RT4 cells: effects on tumorigenic phenotype. (a–c) Gross appearances of RT4 cells inoculated alone and RT4 cells plus fetal mesenchyme (bar = 2 mm). Representative images of H&E stained tissue (d–f), WSS stains (g–i), and αSMA staining (j–l) (bar = 50 μm, magnification = × 400).

irregular shapes (Fig. 5a–c). H&E staining of xenografted tumors revealed that there was little stroma in the tumors, i.e., micropapillary-like structures were not formed in RT4 cells + fetal mesenchyme groups (Fig. 5e and f). Strong staining for WSS was observed in most regions of RT4 cells (Fig. 5g–i) and αSMA-positive smooth muscle or myofibroblasts were not observed (Fig. 5j–l). In RT4 cells + fetal mesenchyme groups, poorly differentiated cancer cells were increased compared to RT4 cells inoculated alone. These cancer cells exhibited pleomorphic nuclei and an increase in nuclear cytoplasmic (N/C) ratio.

3.6. Combining 3 human bladder cancer cell lines with fetal mesenchyme: Effects on tumorigenicity in vivo

In T24 cells + fetal mesenchyme groups, the Ki-67 labeling index was significantly elevated compared to T24 cells inoculated alone (Fig. 6a–c, Table 2). In UM-UC-3

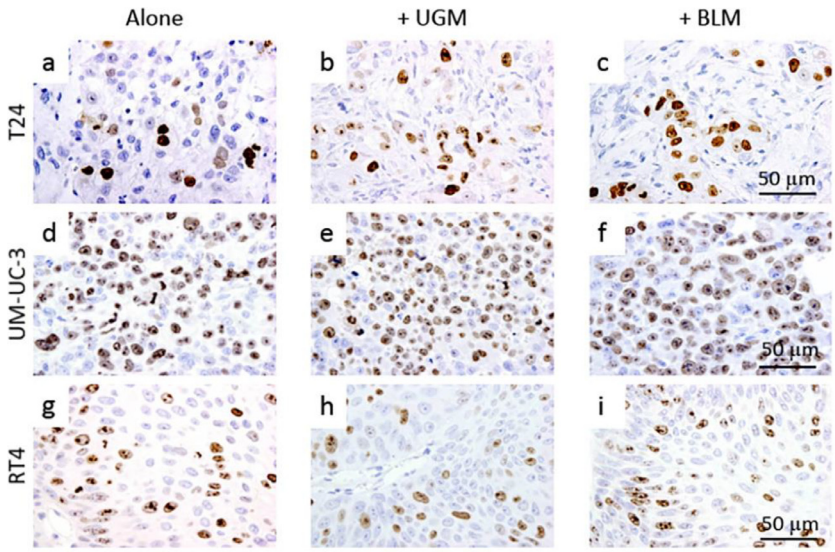

Fig. 6. Combination of fetal mesenchyme with human bladder cancer cells: effects on Ki-67 labeling index in xenografted tumors. Representative images of Ki-67 staining (bar = 50 μm, magnification = × 400) of T24 cells (a–c), UM-UC-3 cells (d–f), and RT4 cells (g–i).

Table 2
Combination of fetal mesenchyme with human bladder cancer cells: effects on Ki-67 labeling index in xenografted tumors

	Ki-67 index (%)		
Cell line	Alone	+ UGM	+ BLM
T24	24.1 ± 9.6	63.2 ± 8.4**	51.7 ± 12.9**
UM-UC-3	65.7 ± 6.7	71.0 ± 11.6	73.1 ± 8.8*
RT4	40.9 ± 10.3	39.2 ± 11.0	39.0 ± 8.7

* $P < 0.05$.
** $P < 0.001$ vs. alone.

Table 3
Combination of fetal mesenchyme with human bladder cancer cells: effects on p63 labeling index in xenografted tumors

	p63 index (%)		
Cell line	Alone	+ UGM	+ BLM
T24	48.4 ± 4.7	64.8 ± 4.6**	66.4 ± 4.8**
UM-UC-3	37.1 ± 4.8	45.6 ± 2.8**	37.2 ± 3.8
RT4	99.0 ± 0.5	99.4 ± 0.5	99.3 ± 0.5

*$P < 0.05$.
** $P < 0.001$ vs. alone.

cells + the UGM group, the Ki-67 labeling index was not altered compared to UM-UC-3 cells inoculated alone (Fig. 6d and e, Table 2). In contrast, the Ki-67 labeling index in UM-UC-3 cells + the BLM group was significantly but slightly elevated (Fig. 6d and f, Table 2). In RT4 cells + fetal mesenchyme groups, the Ki-67 labeling index was not altered compared to RT4 cells inoculated alone (Fig. 6g–i, Table 2).

In T24 cells + fetal mesenchyme groups, the p63 labeling index was significantly elevated compared to T24 cells inoculated alone (Fig. 7a–c, Table 3). In UM-UC-3 cells + the UGM group, the p63 labeling index was significantly but slightly elevated (Fig. 7d and e, Table 3). In contrast, the p63 labeling index in UM-UC-3 cells + the BLM group was not altered compared to UM-UC-3 cells inoculated alone (Fig. 7d and f, Table 3). In RT4 cells + fetal mesenchyme groups, the p63 labeling index was not altered compared to RT4 cells inoculated alone (Fig. 7g–i, Table 3).

4. Discussion

In the treatment of pT1 NMIBC, many clinical and biological parameters identify aggressive pT1 tumors [21]. However, clinicians lack a biomarker for the detection of pT1 NMIBC with a high potential for stage progression. The decision to undertake total cystectomy is predicated in part on the ability to predict invasiveness and metastases. In that regard, it is known that the tumor microenvironment of MIBC can induce the EMT, a feature of cellular detachment. The development of the EMT depends on the responsiveness of cancer cells to stroma and can be observed as micropapillary structures. Thus, micropapillary structures such as tumor budding could be a predictor of poor outcome. In the present study, we mixed 3 established human bladder cancer cell lines (high-grade T24 and UM-UC-3 cells, and low-grade papillary RT4 cells) with fetal rat mesenchyme to evaluate tumorigenic phenotypes in vivo. The histopathological and immunohistochemical analysis demonstrated that each human bladder cancer cell line showed a distinctly different tumorigenic phenotype in their formation of micropapillary-like structures. T24 cells interacted with fetal mesenchyme through formation of micropapillary-like structures and increased proliferation. In contrast, UM-UC-3 and RT4 cells did not form micropapillary-like structures, i.e., they did not respond to fetal mesenchyme and they proliferated by themselves.

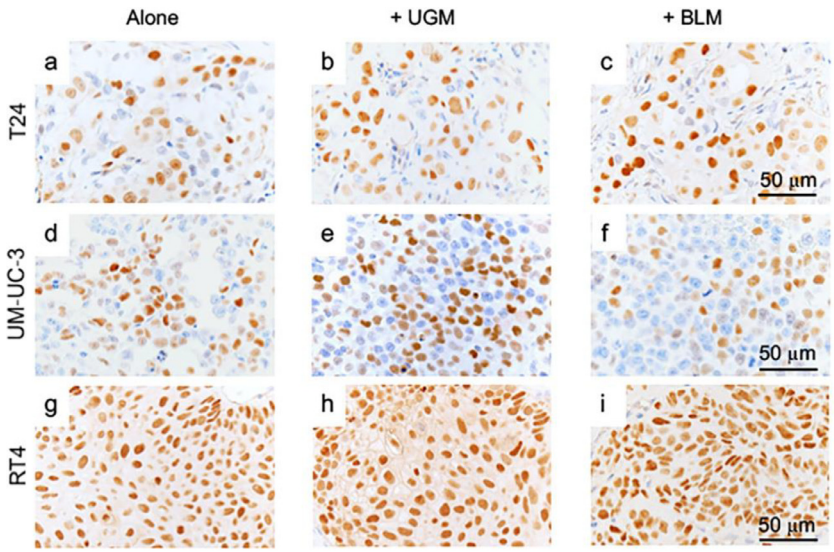

Fig. 7. Combination of fetal mesenchyme with human bladder cancer cells: effects on p63 labeling index in xenografted tumors. Representative images of p63 staining (bar = 50 μm, magnification = × 400) of T24 cells (a–c), UM-UC-3 cells (d–f), and RT4 cells (g–i).

In this study, we used previously established homogenous human bladder cancer cell lines to investigate differences in the formation of micropapillary-like structures. NMIBC cells often grow aggressively by themselves as observed in UM-UC-3 and RT4 tumors but often do not invade muscle. Cancer cells derived from a low-grade papillary human bladder cancer cell line also failed to associate with fibroblastic cell layers or show marked stimulation of growth by preformed layers of fibroblastic cells [10]. On the other hand, cells derived from a patient with highly invasive disease readily infiltrated layers of fibroblasts, a pathological response seen in MIBC [10]. These cells were strongly stimulated to grow by the presence of stromal cells. In this study, UM-UC-3 cells, from high-grade bladder cancer, did not interact with fetal mesenchyme. This observation suggests that the malignant grade of human bladder cancer cell lines cannot predict responsiveness of cancer cells to stroma. Thus, the process of tumorigenesis observed among human bladder cancer cell lines must be analyzed with caution.

In bladder cancer, the EMT has been linked to cellular invasiveness [22,23]. In accordance with the dynamic yet transient morphological and phenotypic alteration of cancer cells during the EMT process, such mesenchymal-transitioned cancer cells are often seen at the invasive front of tumor tissue beside neighboring epithelial cancer cells [24]. Micropapillary structures (composed of mesenchymal-transitioned cancer cells) are often observed at this invasive front of tumor tissue. The tumor microenvironment in co-cultures can activate the EMT, demonstrating the synergistic crosstalk in tumor−stromal interactions [25]. Particularly, transforming growth factor-β signaling is involved in a large number of cellular processes including the EMT [26]. Various EMT-inducing signaling pathways such as transforming growth factor-β and Wnt produced by the surrounding stromal cells are active in micropapillary structures [27,28]. Thus, invasive and metastatic potentials of bladder cancer cells could be influenced by both cancer cell properties and their responsiveness to stroma.

The *TP63* gene, a member of the *TP53* tumor suppressor gene family, can be expressed in at least 6 isoforms due to alternative promoter use and alternative splicing. The two main groups of p63 isoforms include the TA isoforms in which the N-terminal transactivation domain is retained, and the ΔN isoforms which lack the TA domain [29]. However, the lack of p63 isoform-specific antibodies has limited the analysis of the biological significance of p63. The anti-p63 antibodies (clone 4A4) used in this study recognize all p63 isoforms (TAp63α, TAp63β, TAp63γ, ΔNp63α, ΔNp63β, and ΔNp63γ). In our study, Western blot analysis showed that T24 cells expressed one p63 isoform p63γ (TAp63γ or ΔNp63γ) (Fig. 1B). When combined with fetal mesenchyme, only T24 cells responded to fetal mesenchyme and formed micropapillary-like structures (Fig. 3). Further investigations are needed to determine the role of p63 isoforms expressed during bladder cancer progression.

Micropapillary structures such as tumor budding is a predictor of poor outcome in many carcinomas, including colon [4,30], breast [31], pancreatic [32], and oral carcinomas [33]. Similarly, clinical specimens of bladder cancer have been used to assess poor outcomes based on evaluations of tumor budding [6]. The study of tumor−stromal interactions in bladder cancer is at an early stage and many questions remain to be answered. In the present study, our data suggest that the responsiveness of cancer cells to stroma through formation of micropapillary-like structures may be a predictor of poor outcome in invasive bladder cancer. Using a xenograft transplant model, histopathologic examination can predict invasiveness and metastases of human bladder cancer cells by their response to fetal mesenchyme and the presence of micropapillary-like structures, as in T24 cells. In addition, heterospecific combination experiments have a number of technical advantages. Mixing human cancer cells and fetal mesenchyme from different species reinforces the idea that these tissues communicate in ways that can be understood across species barriers [34]. Easily detectable specific markers, for example, expression of p63γ (TAp63γ or ΔNp63γ), which may be related to bladder cancer cell responsiveness to stroma, should predict poor outcome. At present, it is not clear how much impact cancer cells' responsiveness to stroma makes on the ultimate outcome of NMIBC. Further investigations are needed to determine the responsiveness of cancer cells to stroma and the prediction of poor outcome.

Conflict of Interest

The authors have no conflict of interest.

Ethical Approval

All applicable international, national, and/or institutional guidelines for the care and use of animals were followed. This article does not contain any studies with human participants performed by any of the authors.

Acknowledgments

We would like to thank Mrs. Izumi Matsuoka and Miss Yumi Yoshikawa for technical support. We especially appreciate the advice and expertise of Drs. Nobuyuki Oda, Motomu Sakuragi, and Kenjiro Ito from Taiho Pharmaceutical Co., Ltd. A part of this study was performed with Taiho Pharmaceutical Co., Ltd. as a joint research between 2011 and 2014.

References

[1] Kamat AM, Hahn NM, Efstathiou JA, Lerner SP, Malmstrom PU, Choi W, et al. Bladder cancer. Lancet 2016;388:2796–810.

[2] Garg M. Urothelial cancer stem cells and epithelial plasticity: current concepts and therapeutic implications in bladder cancer. Cancer Metastasis Rev 2015;34:691–701.
[3] Tsai JH, Donaher JL, Murphy DA, Chau S, Yang J. Spatiotemporal regulation of epithelial-mesenchymal transition is essential for squamous cell carcinoma metastasis. Cancer Cell 2012;22:725–36.
[4] Hase K, Shatney C, Johnson D, Trollope M, Vierra M. Prognostic value of tumor "budding" in patients with colorectal cancer. Dis Colon Rectum 1993;36:627–35.
[5] Zlobec I, Lugli A. Epithelial mesenchymal transition and tumor budding in aggressive colorectal cancer: tumor budding as oncotarget. Oncotarget 2010;1:651–61.
[6] Fukumoto K, Kikuchi E, Mikami S, Ogihara K, Matsumoto K, Miyajima A, et al. Tumor budding, a novel prognostic indicator for predicting stage progression in T1 bladder cancers. Cancer Sci 2016;107:1338–44.
[7] Miyake M, Hori S, Morizawa Y, Tatsumi Y, Toritsuka M, Ohnishi S, et al. Collagen type IV alpha 1 (COL4A1) and collagen type XIII alpha 1 (COL13A1) produced in cancer cells promote tumor budding at the invasion front in human urothelial carcinoma of the bladder. Oncotarget 2017;8:36099–114.
[8] Gururajan M, Posadas EM, Chung LW. Future perspectives of prostate cancer therapy. Transl Androl Urol 2012;1:19–32.
[9] Pollard JW. Tumour-educated macrophages promote tumour progression and metastasis. Nat Rev Cancer 2004;4:71–8.
[10] Pritchett TR, Wang JK, Jones PA. Mesenchymal-epithelial interactions between normal and transformed human bladder cells. Cancer Res 1989;49:2750–4.
[11] Van Batavia J, Yamany T, Molotkov A, Dan H, Mansukhani M, Batourina E, et al. Bladder cancers arise from distinct urothelial subpopulations. Nat Cell Biol 2014;16:982–91:1-5.
[12] Shin K, Lim A, Odegaard JI, Honeycutt JD, Kawano S, Hsieh MH, et al. Cellular origin of bladder neoplasia and tissue dynamics of its progression to invasive carcinoma. Nat Cell Biol 2014;16:469–78.
[13] Spiess PE, Czerniak B. Dual-track pathway of bladder carcinogenesis: practical implications. Arch Pathol Lab Med 2006;130:844–52.
[14] Karni-Schmidt O, Castillo-Martin M, Shen TH, Gladoun N, Domingo-Domenech J, Sanchez-Carbayo M, et al. Distinct expression profiles of p63 variants during urothelial development and bladder cancer progression. Am J Pathol 2011;178:1350–60.
[15] Cunha GR, Foster B, Thomson A, Sugimura Y, Tanji N, Tsuji M, et al. Growth factors as mediators of androgen action during the development of the male urogenital tract. World J Urol 1995;13:264–76.
[16] Cunha GR, Fujii H, Neubauer BL, Shannon JM, Sawyer L, Reese BA. Epithelial-mesenchymal interactions in prostatic development. I. Morphological observations of prostatic induction by urogenital sinus mesenchyme in epithelium of the adult rodent urinary bladder. J Cell Biol 1983;96:1662–70.
[17] Oottamasathien S, Wang Y, Williams K, Franco OE, Wills ML, Thomas JC, et al. Directed differentiation of embryonic stem cells into bladder tissue. Dev Biol 2007;304:556–66.
[18] Ishii K, Sugimura Y. Identification of a new pharmacological activity of the phenylpiperazine derivative naftopidil: tubulin-binding drug. J Chem Biol 2015;8:5–9.
[19] Ishii K, Imamura T, Iguchi K, Arase S, Yoshio Y, Arima K, et al. Evidence that androgen-independent stromal growth factor signals promote androgen-insensitive prostate cancer cell growth in vivo. Endocr Relat Cancer 2009;16:415–28.
[20] Kanai M, Ishii K, Kanda H, Ogura Y, Kise H, Arima K, et al. Improvement in predicting tumorigenic phenotype of androgen-insensitive human LNCaP prostatic cancer cell subline in recombination with rat urogenital sinus mesenchyme. Cancer Sci 2008;99:2435–43.
[21] Babjuk M, Burger M, Zigeuner R, Shariat SF, van Rhijn BW, Comperat E, et al. EAU guidelines on non-muscle-invasive urothelial carcinoma of the bladder: update. Eur Urol 2013;64:639–53.
[22] McConkey DJ, Choi W, Marquis L, Martin F, Williams MB, Shah J, et al. Role of epithelial-to-mesenchymal transition (EMT) in drug sensitivity and metastasis in bladder cancer. Cancer Metastasis Rev 2009;28:335–44.
[23] Cheng T, Roth B, Choi W, Black PC, Dinney C, McConkey DJ. Fibroblast growth factor receptors-1 and -3 play distinct roles in the regulation of bladder cancer growth and metastasis: implications for therapeutic targeting. PLoS One 2013;8:e57284.
[24] Brabletz T, Hlubek F, Spaderna S, Schmalhofer O, Hiendlmeyer E, Jung A, et al. Invasion and metastasis in colorectal cancer: epithelial-mesenchymal transition, mesenchymal-epithelial transition, stem cells and beta-catenin. Cells Tissues Organs 2005;179:56–65.
[25] Buhrmann C, Kraehe P, Lueders C, Shayan P, Goel A, Shakibaei M. Curcumin suppresses crosstalk between colon cancer stem cells and stromal fibroblasts in the tumor microenvironment: potential role of EMT. PLoS One 2014;9:e107514.
[26] Ikushima H, Miyazono K. TGFbeta signalling: a complex web in cancer progression. Nat Rev Cancer 2010;10:415–24.
[27] Dawson H, Lugli A. Molecular and pathogenetic aspects of tumor budding in colorectal cancer. Front Med (Lausanne) 2015;2:11.
[28] Jensen DH, Dabelsteen E, Specht L, Fiehn AM, Therkildsen MH, Jonson L, et al. Molecular profiling of tumour budding implicates TGFbeta-mediated epithelial-mesenchymal transition as a therapeutic target in oral squamous cell carcinoma. J Pathol 2015;236:505–16.
[29] Yang A, Kaghad M, Wang Y, Gillett E, Fleming MD, Dotsch V, et al. p63, a p53 homolog at 3q27-29, encodes multiple products with transactivating, death-inducing, and dominant-negative activities. Mol Cell 1998;2:305–16.
[30] Betge J, Kornprat P, Pollheimer MJ, Lindtner RA, Schlemmer A, Rehak P, et al. Tumor budding is an independent predictor of outcome in AJCC/UICC stage II colorectal cancer. Ann Surg Oncol 2012;19:3706–12.
[31] Salhia B, Trippel M, Pfaltz K, Cihoric N, Grogg A, Ladrach C, et al. High tumor budding stratifies breast cancer with metastatic properties. Breast Cancer Res Treat 2015;150:363–71.
[32] O'Connor K, Li-Chang HH, Kalloger SE, Peixoto RD, Webber DL, Owen DA, et al. Tumor budding is an independent adverse prognostic factor in pancreatic ductal adenocarcinoma. Am J Surg Pathol 2015;39:472–8.
[33] Angadi PV, Patil PV, Hallikeri K, Mallapur MD, Hallikerimath S, Kale AD. Tumor budding is an independent prognostic factor for prediction of lymph node metastasis in oral squamous cell carcinoma. Int J Surg Pathol 2015;23:102–10.
[34] Hayward SW. Approaches to modeling stromal-epithelial interactions. J Urol 2002;168:1165–72.